

LA-UR- 96-3061

CONF-9609245--1

Los Alamos National Laboratory is operated by the University of California for the United States Department of Energy under contract W-7405-ENG-36.

TITLE: Klystron Beam-Bunching Lecture

AUTHOR(S): B. E. Carlsten

SUBMITTED TO: 1996 US/CERN/JAPAN Accelerator School

MASTER

DISTRIBUTION OF THIS DOCUMENT IS UNLIMITED

By acceptance of this article, the publisher recognizes that the U.S. Government retains a nonexclusive, royalty-free license to publish or reproduce the published form of this contribution, or to allow others to do so, for U.S. Government purposes.

The Los Alamos National Laboratory requests that the publisher identify this article as work performed under the auspices of the U.S. Department of Energy.

Los Alamos Los Alamos National Laboratory
Los Alamos, New Mexico 87545

DISCLAIMER

**Portions of this document may be illegible
in electronic image products. Images are
produced from the best available original
document.**

Klystron Beam-Bunching Lecture

Bruce Carlsten
Los Alamos National Laboratory
Los Alamos, NM 87545, USA

Introduction

Electron beam current modulation (the creation of a train of electron bunches) in a klystron is the key phenomena that accounts for klystron gain and rf power generation. Current modulation results from the beam's interaction with the rf fields in a cavity, and in turn is responsible for driving modulation in the next rf cavity. To understand the impact of the current modulation in a klystron, we have to understand both the mechanism leading to the generation of the current modulation and the interaction of a current-modulated electron beam with an rf cavity. The cavity interaction is subtle, because the fields in the cavity modify the bunching of the beam within the cavity itself (usually very dramatically).

In this lecture, we will establish the necessary formalism to understand klystron bunching phenomena. (This formalism can be used to describe rf accelerator cavity/beam interactions.) This formalism is strictly steady-state, and no transient behavior will be considered.

In particular, we will discuss these concepts relevant to klystron operation:

- (1) General description of klystron operation
- (2) Define beam harmonic current
- (3) Describe how beam velocity modulation induced by an rf cavity leads to current modulation in both the ballistic and space-charge dominated regimes
- (4) Use Ramo's theorem to define the power transfer between a bunched electron beam and the cavity
- (5) General cavity model with external coupling (including an external generator if needed), used to describe the input cavity, idler cavities, and the output cavity, including the definition of beam-loaded cavity impedance.

Although all these components are conceptually straight-forward, there is a fair amount of physics represented in these concepts and in order to derive some elements of the formalism from first principles requires excessive steps. Our approach in the following notes will be to present a self-consistent set of equations describing the

important elements of the beam/cavity interaction in klystrons, and to only derive a few relatively simple steps - derivations for moderately complex formulas will be outlined, and a relatively complex derivation of the self-consistent set of equations can be found in the Appendix. The main goal of this self-consistent model is to provide a mechanism that leads to a quantifiable description of klystron behavior.

I. General Description of Klystron Operation

A klystron is conceptually a simple device, and can be thought of as a dc to rf transformer. DC beam power is relatively easy to generate; a small amount of rf power is transferred to the beam in an input cavity. The beam rf power grows from the interaction with subsequent cavities (by increasing the current modulation as the beam travels downstream), and is extracted in an output cavity.

In Figure 1 we show a schematic of a generic klystron. In this figure, the electron beam travels from left to right. The electron beam current before the input cavity is dc. The input cavity is driven by an external generator so that an oscillatory electric field is set up in the gap between the cavity noses. This axial electric field does work on the electron beam $\left(\int_{\text{gap}} eE_{rf,z} dz \right)$; the electron beam gets accelerated during half of the rf

period and decelerated during the other half of the rf period. (The instantaneous integral of the axial electric field in the cavity gap is known as the gap voltage. The maximum accelerating/decelerating potential seen by the beam is the gap voltage times a geometric factor and a transit time factor, both less than, but close to unity.) Downstream, this velocity modulation results in a current modulation as some of the electrons overtake others. For small velocity modulations, this current modulation is sinusoidal (a typical one is shown in Figure 2a) and for large velocity modulations, this current modulation can become nonlinear (a typical one is shown in Figure 2b). We can assume that the current modulation is zero at the center of the input cavity and increases for a while, reaches a maximum at some distance from the input cavity, and then decreases. A typical input cavity can produce a peak current modulation of 0.1% of the average beam current.

An idler cavity is placed at the location of the maximum beam current modulation. This cavity is driven by the beam modulation to a gap voltage much higher than that in the input cavity. The beam velocity is thus modulated by this cavity, and additional current modulation is generated downstream of this cavity. A typical value for the current modulation after the first idler cavity is 1% of the average beam current.

A second and third idler cavities are shown in Figure 1 also, each placed at the location of the maximum beam current modulation from the preceding cavity. The beam current modulation after these cavities can be 10% and 100% of the average beam current. After the final idler cavity, the electron beam has become a train of well-defined bunches, separated by essentially empty space. In the next section, we will learn how to quantify the terms "bunch" and "empty space." Finally, an output cavity is placed at the location of the maximum beam current modulation from the final idler cavity. This cavity is tuned such that the fields induced in it by the beam current modulation oppose the motion of the bunch, and it is decelerated and the power lost from it is extracted from the cavity through an external waveguide.

Often, one or more "penultimate" cavities are introduced just before the output cavity. The purpose of these cavities is to further bunch and increase the harmonic current at the location of the output cavity, to a level unattainable by a single cavity. A typical way to do this is by detuning a cavity relatively far above resonance (known as "inductively tuning"). This will cause the zero of this cavity's fields to be phased near the maximum in the harmonic current, and the cavity fields will then "squish" the bunch further, thereby increasing the harmonic current. Another trick used to increase the harmonic current at the location of the output cavity is to include a cavity resonating at the second harmonic of the operating frequency before the penultimate cavity. This second harmonic cavity will create two smaller bunches per rf period; the penultimate cavity will then be used to merge this two smaller bunches into one larger bunch. Both of these tricks essentially introduce nonlinear beam modulation in order (1) to increase the harmonic current and (2) to increase the axial range over which there is a large harmonic current. This process is the major element in klystron design, and is responsible for increasing the output efficiency (defined by the rf output power divided by the beam power) from a nominal 25-30% to 50-60%, for high-power klystrons. At the location of the output cavity (but with the output cavity not present), harmonic currents of 160% of the beam current are common; with the output cavity present, the harmonic current will typically drop to about 100% of the beam current. The output cavity voltage is typically 1.2-1.3 times the beam voltage.

In later sections of this lecture note, we will present formulas which allow us to quantify the effects of cavity fields on beam bunching, and on beam loading, induced current, and other aspects of beam-cavity interaction physics related to the beam-current modulation. However, in general, numerical solution of these formulas is required because of the inherent nonlinearity of the problem.

II. Definition of Beam Harmonic Current

Although the beam harmonic current is not directly useful for determining how much a cavity is modulated, it is used as a common figure of merit, and can give a reasonable estimate of the extraction efficiency. The harmonic current is defined in terms of the Fourier expansion of the beam current I at a given axial location,

$$I(z, t) = I_0 + I_1(z)\cos(\omega t + \phi_1) + I_2(z)\cos(2\omega t + \phi_2) + \dots \quad (1)$$

where the drive frequency is $f = \omega / 2\pi$ and the average beam current is given by I_0 . When one refers to the harmonic current, one is usually talking about the fundamental harmonic component of the harmonic current, I_1 . This component can range from zero to twice the average beam current (this is easily verified by calculating the coefficient for the harmonic current for a periodic delta function of current). The product $\frac{1}{2}I_1V_0$ is often referred to as the beam rf power, where V_0 is the beam kinetic voltage. The n^{th} Fourier component of the beam current is given by

$$I_n = \sqrt{C_n^2 + S_n^2} \quad (2)$$

where the coefficients C_n and S_n are given by

$$C_n(z) = 2 \int_0^{2\pi} I(t, z) \cos(n\omega t) d(\omega t) \quad (3)$$

$$S_n(z) = 2 \int_0^{2\pi} I(t, z) \sin(n\omega t) d(\omega t)$$

In these definitions, we are keeping the Fourier components of the beam current real, because the beam current is physical and thus real. When we later use the induced current model for cavity excitation, we will introduce complex currents (the induced current is not physically measurable).

We can see how the fundamental harmonic current can be used to estimate the maximum rf power extraction efficiency by using simple power considerations. The power extracted in the output cavity is given by (this is essentially the instantaneous work the rf fields do on the electron beam)

$$P(t) = \int_V \vec{J}(\vec{r}, t) \cdot \vec{E}_{rf}(\vec{r}, t) dV, \quad (4)$$

where \vec{J} is from the beam current and \vec{E}_{rf} is from the cavity's fields, which we will assume have a $\cos(\omega t)$ time dependence. Only the fundamental Fourier component leads to a nonzero contribution, and if we assume that the cavity is phased to extract the most power and that the cavity fields only extend over a very short axial distance, the average extracted power reduces to $P_{ave} = \frac{1}{2} I_1 V_{gap} M$, where M is a transit-time factor, and the gap voltage is defined as the line integral of the electric field along some path S of interest,

$$V_{gap} = \int_S \vec{E}(\vec{r}) \cdot d\vec{l} \quad (5)$$

For optimal performance, the output cavity gap voltage is very nearly the same as the beam voltage, so the extraction efficiency is about $\eta = (1/2) I_1 / I_o$. Note that a train of delta function bunches ($I_1 = 2I_o$) gives a maximum extracted power of $I_o V_o$ (the same as the dc beam power), which is what we would intuitively expect.

III. Bunching due to Beam Velocity Modulation

In this section, we will present formulas that describe the beam harmonic current evolution as a function of axial position downstream from a cavity which imposes a velocity modulation on the beam and as a function of the cavity gap voltage.

Space-charge dominated bunching

The growth of the beam harmonic current can be either space-charge dominated or ballistic, depending on the current, and the modulation voltage. In addition, it can also be either small- or large-signal. For small momentum modulations, the bunching in the space-charge-dominated regime results from space-charge compression waves initiated by the cavity. The current modulation from this effect is given by

$$\frac{I_1}{I_o} = \frac{1}{(1+\gamma)\gamma^{3/2}} \frac{\omega}{\omega_q} \frac{V_{gap}}{V_o} T , \quad (6)$$

where T is the transit time factor

$$T = \frac{\sin\left(\frac{\omega d}{2v_0}\right)}{\left(\frac{\omega d}{2v_0}\right)} \quad (7)$$

for a gap of length d , where v_0 is the dc beam velocity and ω_q is the reduced plasma frequency, given by $\omega_q = R \sqrt{\frac{e\rho_o}{mc}}$, where now e is the electronic charge, m is the electronic mass, ρ_o is the dc charge density in the beam, c is the speed of light, and R is the reduction factor. For modern, high-perveance klystrons, ω_q can actually become larger than ω (this provides additional complications in the space-charge bunching which we will not consider).

The maximum harmonic modulation occurs at an axial distance from the cavity of

$$z_b = \frac{\pi v_0}{2\omega_q \gamma^{3/2}} \quad (8)$$

This space-charge dominated bunching can be analytically evaluated by considering the equation for the rf axial space-charge electric field due to a density modulation, the Lorentz force equation (which shows how the time and axial derivatives of the rf beam velocity is related to the rf axial electric field), and the continuity equation (which can be used to relate the rf velocity to the rf density). Note that the maximum harmonic current is always very low from space-charge bunching.

Now we will summarize the analysis leading to Eqns. (7) and (8), assuming 1-D symmetry for simplicity. A full 3-D analysis will lead to qualitatively the same results because klystrons typically have heavily confined flow (a large axial magnetic field is applied which constrains the electrons to move only axially). This analysis will be Eulerian, or fluid in nature. We will consider the charge density, current density, and velocity of a small, continuous element of the beam. In this analysis, we will assume the dc electron density is given by N , the dc charge density is given by ρ_o , the dc current density is given by J_o , and the dc beam velocity is v_0 . The rf number density will be

called n , the rf charge density will be called ρ , the rf current density will be called J , and the rf beam velocity will be called v , and the rf axial electric field will be called E . We will assume all rf components have an implicit $e^{j\omega t}$ time dependence.

The Lorentz force equation for a small element of the beam then becomes

$$(N+n)\frac{d}{dt}\gamma v = (\rho - \rho_o)E. \quad (9)$$

To lowest order we can ignore the rf number density and rf charge density, and after expanding the total derivative in terms as a convective derivative, using the assumed time dependence, and using $\frac{d\gamma}{dv} = \gamma^3 \frac{v}{c^2}$, we end up with

$$v = \frac{-(e/m)E/\gamma^3}{j\omega - j\beta v} \quad (10)$$

The definition of the total current density is

$$(J_o + J) = (\rho - \rho_o)(v + v_o) \quad (11)$$

and the rf current density to lowest order is

$$J = \rho v_o - \rho_o v \quad (12)$$

The continuity equation also gives

$$\frac{\partial J}{\partial z} = -j\omega \rho \quad (13)$$

At this time, we will also assume an $e^{-j\beta z}$ axial dependency (this is the space-charge wave assumption), and the continuity equation becomes

$$\beta J = \omega \rho \quad (14)$$

Using Eqns. (12) and (14) to find another equation for v we find

$$J(\omega - \beta v_o) = -\omega \rho_o v \quad , \quad (15)$$

which, with Eqn. (10) gives

$$J = j \frac{\omega_p^2 \beta_o^2 \epsilon E / \gamma^3}{\omega (\beta_o - \beta)^2} \quad (16)$$

where we have defined $\beta_o = \omega / v_o$. We now will get a second relation between J and E by using the equation for the vector potential resulting from a current density, and set these two expressions equal, and end up with a dispersion relation for the axial propagation constant β .

The wave equation for the axial vector potential is

$$\nabla^2 A_z + k_o^2 A_z = -\mu J \quad (17)$$

where we are using $k_o = \omega / c$. Using the Lorentz gauge, the electric field in terms of the vector potential is

$$E = -j\omega A_z + \frac{\partial}{\partial z} \left(\vec{\nabla} \cdot \vec{A} \right) = \frac{k_o^2 - \beta^2}{j\omega \mu \epsilon} A_z \quad . \quad (18)$$

Combining Eqns. (17) and (18) we find

$$E = -\frac{J}{j\omega \epsilon} \quad . \quad (19)$$

Combining this equation with Eqn. (16) we finally arrive at the dispersion relation for β :

$$(\beta_o - \beta)^2 = \gamma^3 \frac{\omega_p^2}{\omega^2} \beta_o^2 \quad , \quad (20)$$

which has solution

$$\beta_{\pm} = \beta_o \left(1 \pm \frac{\omega_p}{\omega} \gamma^{3/2} \right) \quad . \quad (21)$$

The usual approach at this point is to write

$$J = Ae^{-j\beta_+ z} + Be^{-j\beta_- z} \quad (22)$$

and to set $J = 0$ at $z = 0$ in order to evaluate the coefficients. This is not strictly true (really only the charge density vanishes at $z = 0$), but is a good approximation if ω_p is much less than ω (if this is not valid, the current modulation will end up having two wave components). This immediately gives $B = -A$, and

$$J = -2Aje^{-j\beta_o z} \sin\left(\frac{\omega_p}{\omega} \gamma^{3/2} \beta_o z\right). \quad (23)$$

Using the equation for the rf current density and the continuity equation (Eqn. (13), not Eqn. (14)), we find

$$v = Aj \frac{2v_o}{\omega \rho_o} \left(\frac{\omega_p}{\omega} \gamma^{3/2} \beta_o \right) e^{-j\beta_o z} \cos\left(\frac{\omega_p}{\omega} \gamma^{3/2} \beta_o z\right). \quad (24)$$

Now note that the velocity modulation from a cavity with gap voltage V_{gap} is given by

$$v(z=0) = \frac{eV_{gap}T}{(\gamma^2 - 1)\gamma mc^2} v_o \quad (25)$$

which immediately gives us

$$A = \frac{eV_{gap}T v_o \rho_o}{j2(\gamma^2 - 1)\gamma^{5/2} mc^2} \frac{\omega}{\omega_p} \quad (26)$$

and

$$J = -\frac{eV_{gap}T v_o \rho_o}{(\gamma^2 - 1)\gamma^{5/2} mc^2} \frac{\omega}{\omega_p} e^{j(\omega t - \beta_o z)} \sin\left(\frac{\omega_p}{\omega} \gamma^{3/2} \beta_o z\right), \quad (27)$$

where we have now explicitly included the time dependence, and which gives the results reported in Eqns. (6) and (8) (the reduced plasma frequency arises from using a reduced axial electric field in the Lorentz force equation). In Fig. 3 we show a plot of the plasma frequency reduction factor of a solid beam as a function of beam-pipe radius, beam radius and beam velocity. The factor $\omega b / v_o$ is typically about 0.5.

Ballistic bunching

In the limit of vanishing current, or large energy modulation from the cavity, the space-charge forces can be ignored, and the motion is ballistic, with faster particles overtaking slower ones. Ballistic motion is well known for the short-gap, nonrelativistic limit, and always leads to large-signal bunching. For a relativistic beam without space charge, the harmonic current in the limit of a small gap voltage (or equivalently short gap) is

$$I_1 = 2I_0 J_1(\chi) \quad (28)$$

where

$$\chi = \frac{TV_{\text{gap}}e}{mc^2\gamma(\gamma^2-1)} \frac{\omega}{v_o} z \quad (29)$$

Purely ballistic bunching eventually grows to large signal. The harmonic current has a maximum of $1.164 I_0$ at $\chi = 1.84$. These ballistic equations can be easily found by explicitly following trajectories of particles at different phases after the rf cavity, neglecting space-charge forces.

We can derive Eqns. (28) and (29) by following the ballistic trajectories from a gap to a downstream axial location. For simplicity, we will consider a very thin gap, with a small-signal gap voltage. The exit velocity from the gap for a particle passing through at a time t_o is then given by

$$v_{\text{exit}} = v_o \left(1 + \frac{TeV_{\text{gap}}}{\gamma(\gamma^2-1)mc^2} \sin(\omega t_o) \right) \quad (30)$$

This particle will reach a location l downstream at a time t given to lowest order in the gap voltage by

$$\omega t - \omega t_o = \frac{\omega l}{v_o} - \frac{\omega l}{v_o} \frac{TeV_{gap}}{\gamma(\gamma^2 - 1)mc^2} \sin(\omega t_o) . \quad (31)$$

In Fig. 4, we plot the arrival time versus the exit time. The arrival time is single-valued as long as $\frac{\omega l}{v_o} \frac{TeV_{gap}}{\gamma(\gamma^2 - 1)mc^2} < 1$. Note that if the arrival time is single-valued the instantaneous current at $z = l$ is given by

$$I(t) = -I_o \frac{dt_o}{dt} . \quad (32)$$

We can Fourier decompose the current at $z = l$ by

$$I(t) = -I_o + \sum_{n=1}^{\infty} a_n \cos(n(\omega t - \theta)) + b_n \sin(n(\omega t - \theta)) \quad (33)$$

where

$$a_n = \frac{1}{\pi} \int_{\theta-\pi}^{\theta+\pi} I(t) \cos(n(\omega t - \theta)) d(\omega t) \quad (34)$$

$$b_n = \frac{1}{\pi} \int_{\theta-\pi}^{\theta+\pi} I(t) \sin(n(\omega t - \theta)) d(\omega t) .$$

Let us consider the case that the arrival time is single-valued, where we can use

$$I(t) d(\omega t) = -I_o d(\omega t_o) . \quad (35)$$

The coefficients a_n and b_n become

$$a_n = -\frac{I_o}{\pi} \int_{-\pi}^{\pi} \cos(n(\omega t_o - \chi \sin \omega t_o)) d(\omega t_o) = -2I_o J_n(n\chi) \quad (36)$$

$$b_n = -\frac{I_o}{\pi} \int_{-\pi}^{\pi} \sin(n(\omega t_o - \chi \sin \omega t_o)) d(\omega t_o) = 0$$

and the current at $z = l$ becomes

$$I(t) = -I_o - 2I_o \sum_{n=1}^{\infty} J_n(n\chi) \cos(n(\omega t - \theta)) \quad (37)$$

which gives us the results in Eqns. (28) and (29).

For axial positions where the arrival time is multi-valued, the Fourier integral has to be broken into different time intervals that are single-valued; after doing so, the exact same expressions for the coefficients a_n and b_n results. The time (arrival and exit) values that define these intervals are shown in Fig. 4.

Nonlinear bunching (using either a second harmonic cavity or a penultimate cavity) cannot be adequately described by either the small-signal or the ballistic representation, and can only be calculated with numerical simulations. Also, for single cavity modulation, the beam harmonic current evolution in the regime between pure space-charge bunching and ballistic bunching can only be numerically evaluated. It should also be noted that significant second harmonic bunching can occur if the beam can execute at least 1/3 of a reduced plasma oscillation between idler cavities.

IV. Ramo's Theorem for Power Transfer from a Bunched Beam to the Cavity

A bunched beam will drive an rf cavity, causing a nonzero gap voltage. This gap voltage will in turn modify the bunch structure within the cavity itself. In this section, we present the self-consistent model for steady-state cavity excitation by a current modulated beam (including the effect of external coupling). This interaction model uses a fictitious current, called the induced current, to mediate the interaction. The fundamental Fourier component of this current will be denoted by i_1 to distinguish it from the very physical (but not as useful) fundamental Fourier component of the beam current, I_1 .

The cavity model, the external coupling model, the induced current model and the match model all assume a steady-state condition has been reached. In Fig. 5 we present the circuit model for the input cavity. The internal cavity impedance, Z_{cav} , is given either in terms of the cavity shunt impedance R , the cavity capacitance C , the cavity inductance L , or alternatively in terms of R , the cavity resonant frequency f_o , the operating frequency f , and the cavity R/Q factor by

$$\begin{aligned}\frac{1}{Z_{cav}} &= \frac{1}{R} + j\omega C + \frac{1}{j\omega L} \\ &= \frac{1}{R} + j\left(\frac{f}{f_o} - \frac{f_o}{f}\right) \frac{1}{R/Q} ,\end{aligned}\quad (38)$$

where the two definitions are related by $R/Q = 1/2\pi f_o C$ and $(2\pi f_o)^2 CL = 1$. The cavity gap voltage is defined as the line integral of the electric field along some path S of interest, defined in Eqn. (5), and is the voltage across the cavity impedance in Fig. 5, given by

$$V_{gap} = Z_{cav}(i + i_1) , \quad (39)$$

where i is the current in the cavity circuit due to the generator and i_1 is the current in the cavity circuit due to the beam, usually known as the beam induced current. For typical input cavities of conventional klystrons, the induced current counters most of the generator drive and the resulting gap voltage is much smaller than the absolute value of $|iZ_{cav}|$. The induced current physically arises from the slight bunching of the electron beam within the cavity fields, as it reaches the downstream end of cavity, which then feeds back and induces a counter drive to the cavity fields. For klystron cavities, the path S in Eqn. (5) is typically taken along the axis from $z = -\infty$ to $z = \infty$. The cavity shunt impedance is defined from the power P required to establish a modulation V_{gap} in the cavity:

$$R = \frac{V_{gap}^2}{2P} . \quad (40)$$

Since the cavity Q is also defined in terms of the power required to establish a given cavity modulation, the ratio of the shunt impedance to the cavity Q is independent of power, and is just a geometrical factor,

$$\frac{R}{Q} = \frac{\left(\int_S \vec{E}(\vec{r}) \cdot d\vec{l} \right)^2}{\omega e \int_V |\vec{E}(\vec{r})|^2 d\vec{r}} , \quad (41)$$

where the volume integral is taken over the cavity volume.

The model is completed by using Ramo's theorem to define the instantaneous induced current i_{ind} ,

$$i_{ind}(t) = \frac{\int_V \vec{J}(t) \cdot \vec{E}_rf(t) d\vec{r}}{V_{gap}(t)} . \quad (42)$$

Eqn. (38) defines the cavity impedance, Eqn. (39) defines the relation between the induced current, cavity impedance, and the gap voltage, and Eqn. (42) defines the induced current in term of the gap voltage. These three equations define a self-consistent description of a beam/cavity interaction, in which the induced current drives the gap voltage, but the gap voltage in turn effects the induced current.

From Eqns. (38) and (39) we can determine useful phasing information of the gap voltage. If the cavity is tuned on resonance (defined by $f = f_o$), the cavity impedance is purely real. For all cavities other than the input cavity (and for the output cavity in particular), the internal generator current i is zero, and for resonant tuning, the gap voltage is then in phase with the induced current. From the definition of the gap voltage in Fig. 5, we see that this means that the gap voltage *decelerates* the bunch represented by the induced current, and the maximum amount of power is extracted from it. This is usually the tuning desired in the output cavity. Note that in an output cavity, the beam harmonic current is comparable to the average beam current, as is the gap voltage to the beam voltage. Thus, the cavity shunt impedance (including the loading to an external waveguide) must be comparable to the beam impedance. For typical klystrons, the unloaded cavity shunt impedance is several orders of magnitude higher than the beam impedance, and the cavity must be heavily loaded by the external coupling. (In the Appendix, it is shown that the proper shunt impedance to use in Eqn. (38) is the externally loaded cavity shunt impedance, defined by the cavity R/Q times the loaded cavity Q .)

Also, we can consider the case of a penultimate cavity, where we want to further compress an existing bunch. If the cavity resonant frequency is higher than the rf frequency, the cavity impedance has a negative complex phase (which is typically very near $-\pi/2$). In this case, the phase of the gap voltage is such that the gap voltage vanishes for the center of the arriving bunch, accelerates electrons behind the center, and decelerates electrons in front of the center, thereby further compressing the bunch. Note that as the detuning is increased, the cavity impedance drops from several orders of magnitude larger than the beam impedance (at zero detuning) to a level comparable to the beam impedance, and even smaller for extremely high detunings. Thus, even for large-signal beam current modulations, a penultimate cavity can be used to further compress the bunch with a gap voltage not exceeding the beam voltage.

For maximum gain, idler cavities are typically tuned right on resonance. From Eqn. 6, we see that the gain (ratio of one idler cavity gap voltage to the previous idler cavity gap voltage) is given approximately by $(I_o Z_{cav} / V_o)(\omega / \omega_q)/2$, which is typically on the order of 10 (for high-perveance designs) to 100 (for low-perveance designs). For example, a typical cavity impedance at L-band is $2(10^5) \Omega$ and a high power tube may be designed with a beam voltage of $2(10^5) \text{ V}$ and an average current of 100 A, and with a reduced plasma frequency of 1-2 GHz.

V. General Cavity Model with External Coupling

Using the model defined in the previous section, we can determine all sorts of useful, quantitative features of the beam/cavity interaction. In this section, we will also define the concept of the beam-loaded cavity impedance, which is often used to approximate the beam/cavity interaction in an input cavity. We are also particularly interested in determining the driving power requirements for the input cavity (in terms of the externally loaded cavity Q and the cavity resonant frequency), as the input cavity is the most difficult of all the cavities to analytically describe.

We'll start by examining the externally drive line in the circuit model in Fig. 5. The external waveguide supports both an ingoing wave with current i_g and voltage $i_g Z_o$ and an outgoing wave with current $-i_r$ and voltage $i_r Z_o$. The outgoing wave can be thought of as the combination of part of the drive wave from the generator reflected at the waveguide/cavity boundary and power being drained from the internal cavity modulation. It is typically fully absorbed in a circulator load and is thus isolated from the generator itself. The waveguide and the cavity are coupled through a mutual inductance M ; the self-inductance of the cavity is included in the cavity impedance and any stray self-

inductance of the waveguide in the waveguide-cavity coupling is ignored. This assumption is not limiting, because the stray self-inductance of the waveguide only leads to a slight effective detuning of the cavity's resonant frequency, with no other effect for a high Q cavity.

Using Fig. 5 and the definition of the mutual inductance, we have these expression for the currents in the cavity-waveguide circuit:

$$i_g + i_r = \frac{j\omega M}{Z_0} i \quad (43)$$

and

$$-i_g + i_r = (i + i_1) \frac{Z_{cav}}{j\omega M} \quad (44)$$

where as before $\omega = 2\pi f$ is the radian operating frequency and Z_0 is the waveguide characteristic impedance. Since we will assume that the generator current within the cavity i is given and the induced current i_1 can be calculated as discussed in the previous section, these two equations are sufficient to define all other parameters.

Externally loaded cavity Q

First, we will find the externally loaded cavity Q , in the absence of the electron beam and with the external generator off. We assume the cavity has some modulation (possibly from by the current drive i) and some losses both internal and in the external waveguide. The cold externally loaded cavity Q is then defined by

$$Q_l = \frac{\omega E_{stored}}{2P_{loss}} \quad (45)$$

where E_{stored} is the stored energy in the cavity,

$$E_{stored} = \frac{1}{2} \frac{1}{\omega^2 C} |i_C|^2 + \frac{1}{2} L |i_L|^2 , \quad (46)$$

where i_C is the current through the capacitor and i_L is the current through the inductor, and the power loss is

$$P_{loss} = \frac{1}{2} R |i_R|^2 + \frac{1}{2} Z_o |i_r|^2 \quad (47)$$

where $|i_R|$ is the current through the resistor in the cavity circuit model. Using the circuit model in Fig. 5, we find that the loaded cavity Q without beam is given by

$$Q_l = Q_o \frac{1}{1 + \text{Re}(\beta)} , \quad (48)$$

where the unloaded cavity Q is given by

$$Q_o = \frac{\omega C R}{2} \left(1 + \frac{1}{\omega^2 C L} \right) \quad (49)$$

and we have defined a complex coupling coefficient β to be

$$\beta = \frac{Z_o Z_{cav}}{\omega^2 M^2} \quad (50)$$

for convenience. Note that Z_o and M are real; β and Z_{cav} have the same complex phase angle.

Power required from the generator

The generator must supply a power

$$P_g = \frac{1}{2} Z_o |i_g|^2 . \quad (51)$$

Eliminating the generator current in terms of the induced current and gap voltage, we find this formula for the power supplied by the generator:

$$P_g = \frac{1}{8} |1 + \beta|^2 \frac{\left| V_{gap} - \frac{i_1 Z_{cav}}{1 + \beta} \right|^2}{|Z_{cav}| |\beta|} , \quad (52)$$

which is accurate for an arbitrary cavity-waveguide coupling β . The induced current drive is only a function of the gap voltage, and can be expressed by

$$i_l = V_{gap} / Z_b , \quad (53)$$

where the beam impedance Z_b is essentially independent of the gap voltage (as long as the modulation is small signal), and can be easily found numerically (various analytic expressions for Z_b exists, but they are unreliable). We can write the power required from the generator as

$$P_g = \frac{1}{8} |1 + \beta|^2 \frac{|V_{gap}|^2}{|Z_{cav}| |\beta|} \left| 1 - \frac{Z_{cav}}{(1 + \beta) Z_b} \right|^2 . \quad (54)$$

Using the concept of the beam impedance, we can use Fig. 6 as an alternative circuit model for small-signal operation, which is now independent of the induced current. The total impedance of the cavity (the beam-loaded cavity impedance) is now given by $(1/Z_b + 1/Z_{cav})^{-1}$. This concept of a beam-loaded impedance only requires small-signal operation, and is valid in both the input cavity and also small-signal idler cavities. The beam impedance is almost always much smaller than the cavity impedance, and thus the beam-loaded cavity impedance is very close to the beam impedance.

Special case of matched coupling

The coupling is matched if there is no reflected wave when the beam is present. This case is desirable because it leads to the least amount of power from the generator for achieving a desired cavity modulation. In this section, we will determine the match condition on the coupling parameter β , the power from the generator for a matched coupling, and expressions for the cavity detuning and cold externally loaded Q that lead to the proper match. Because β and the unloaded cavity impedance have the same complex phase, not all unloaded cavity impedances can be matched; the input cavity resonant frequency must be detuned to the proper value.

If the coupling is matched, we find

$$\beta = \frac{Z_b - Z_{cav}}{Z_b} , \quad (\text{Match condition}) \quad (55)$$

Eqn. (27) for the power from the generator can in turn be rewritten as

$$P_g = \frac{1}{2} |V_{gap}|^2 \left| \frac{Z_{cav} - Z_b}{Z_b Z_{cav}} \right| . \quad (\text{Match condition}) \quad (56)$$

This expression is certainly not surprising since the last term is the beam-loaded cavity admittance shown in Fig. 6. Note that the cavity impedance Z_{cav} is typically large and mostly positive and, with the sign convention used to define the beam impedance, Z_b is small and mostly negative. Thus, the beam-loaded cavity admittance is essentially the beam admittance, and the unloaded cavity impedance does not influence it as long as it is sufficiently large.

Now let us find an explicit formula for the cavity detuning and cold externally loaded Q that will lead to a matched coupling.

By comparing the definition of the coupling coefficient β from Eqns. (50) and (55) we see

$$\omega^2 M^2 = \frac{Z_o}{1/Z_{cav} - 1/Z_b} . \quad (\text{Match condition}) \quad (57)$$

The left-hand side of this equation is real; the left-hand side depends on the resonant frequency f_o and can be made real by the proper choice of the resonant frequency. Note that for a given cavity design, the cavity shunt impedance and R/Q factor are essentially fixed, and that finding the detuning which leads to a real right-hand side of Eqn. (57) uniquely determines the unloaded cavity impedance. If we define a fractional detuning by $(\delta + 1)f = f_o$ (δ is positive for a cavity resonant frequency greater than the operating frequency), we see that the cavity detuning must be

$$\delta = -\frac{R/Q}{2} \text{Im}(1/Z_b) \quad (\text{Match condition}) \quad (58)$$

in order to satisfy the match condition.

Once the cavity impedance is found using this detuning, the externally loaded cavity Q without beam is given by (using Eqn. (48))

$$Q_l = Q_o \frac{1}{1 + \operatorname{Re} \left(\frac{Z_b - Z_{cav}}{Z_b} \right)} . \quad (\text{Match condition}) \quad (59)$$

Equations (58) and (59) together define the requirements for matching the input cavity with the electron beam.

If the beam impedance is purely real (and thus the match cavity tuning is on resonance from Eqn. (58)), and is much smaller than the unloaded cavity impedance, the right-hand-side of Eqn. (59) reduces to the beam-loaded cavity Q in the absence of any external coupling. Thus, for a purely real beam impedance much smaller than the unloaded cavity impedance, the waveguide coupling is matched when the beam is present if the externally loaded Q without beam equals the beam-loaded cavity Q in the absence of the waveguide coupling.

If the matching conditions are not satisfied, Eqn. (54) can be used to find the power from the generator for achieving a desired cavity modulation. The coupling parameter β is fixed by the choice of the detuning and the measured cold externally loaded cavity Q (assuming the cavity R/Q factor and shunt impedance are unchanged), and is given by

$$\beta = \frac{Z_{cav}}{\operatorname{Re}(Z_{cav})} \left(\frac{Q_o}{Q_l} - 1 \right) . \quad (60)$$

APPENDIX

In this appendix, we (1) derive Ramo's theorem for periodic current drives and arbitrary cavity loadings and (2) show that Ramo's theorem is consistent with the parallel circuit model in Fig. 5 and with the definition of the cavity impedance (Eqn. (38)) and the cavity gap voltage (Eqn. (39)).

Ramo's theorem is usually derived from nonrelativistic energy conservation arguments, or with the assumption of a sinusoidal current drive and high Q cavities. Here Ramo's Theorem is derived exactly from the normal mode expansion of fields in a cavity driven by a periodic current source, with arbitrary unloaded-cavity and externally loaded-cavity Q s.

In general, at any time t , the electric and magnetic fields can be expressed as

$$\begin{aligned}\vec{E}(\vec{r}, t) &= \sum_m C_m \vec{F}_m(\vec{r}) + \sum_m D_m \vec{E}_m(\vec{r}) \\ \vec{H}(\vec{r}, t) &= \sum_m L_m \vec{G}_m(\vec{r}) + \sum_m K_m \vec{H}_m(\vec{r})\end{aligned}\quad (\text{A1})$$

where the coefficients are in general functions of time, and where \vec{F}_n and \vec{G}_n are the electric and magnetic irrotational fields and \vec{E}_n and \vec{H}_n are the electric and magnetic solenoidal fields satisfying the boundary conditions. In addition, we choose the normalization

$$\begin{aligned}\vec{H}_n &= \frac{1}{k_n} \vec{\nabla} \times \vec{E}_n \\ \vec{E}_n &= \frac{1}{k_n} \vec{\nabla} \times \vec{H}_n\end{aligned}\quad (\text{A2})$$

and the eigenfrequency k_n is the same for both \vec{E}_n and \vec{H}_n .

The periodic current source can be described in a Fourier series

$$\vec{J}(\vec{r}, t) = \sum_n \vec{J}_n(\vec{r}) e^{jn\omega t} \quad (\text{A3})$$

Because Maxwell's equations are linear and time invariant, we can likewise Fourier decompose the steady-state electric and magnetic fields with no loss of generality (since the output of linear, time-invariant, systems has the same exponential time behavior as the input):

$$\begin{aligned}\vec{E}(\vec{r}, t) &= \sum_{m,n} C_{m,n} \vec{F}_m(\vec{r}) e^{jn\omega t} + \sum_{m,n} D_{m,n} \vec{E}_m(\vec{r}) e^{jn\omega t} \\ \vec{H}(\vec{r}, t) &= \sum_{m,n} L_{m,n} \vec{G}_m(\vec{r}) e^{jn\omega t} + \sum_{m,n} K_{m,n} \vec{H}_m(\vec{r}) e^{jn\omega t}\end{aligned}\quad (\text{A4})$$

What we are really interested in is calculating the coefficient $D_{m,n}$ because the cavity TM modes are \vec{E}_m modes. We start with the Maxwell curl equations for the n^{th} harmonic, and using the mode orthogonalities, we find:

$$\begin{aligned}
\bar{E}_n &= -\frac{1}{jn\omega\epsilon} \sum_m \frac{\int_V \bar{J}_n \cdot \bar{F}_m dV}{\int_V |\bar{F}_m|^2 dV} \bar{F}_m \\
&\quad + \sum_m \left[\frac{\oint_S (\hat{n} \times \bar{E}_n) \cdot \vec{\nabla} \times \bar{E}_m dS}{(k_m^2 - n^2 k^2) \int_V |\bar{E}_m|^2 dV} - \frac{jn\omega\mu}{(k_m^2 - n^2 k^2)} \frac{\int_V \bar{J}_n \cdot \bar{E}_m dV}{\int_V |\bar{E}_m|^2 dV} \right] \bar{E}_m \\
\bar{H}_n &= \frac{1}{jn\omega\mu} \sum_m -\frac{\oint_S (\hat{n} \times \bar{E}_n) \cdot \bar{G}_m dS}{\int_V |\bar{G}_m|^2 dV} \bar{G}_m \\
&\quad + \sum_m \left[\frac{k_m \int_V \bar{J}_n \cdot \bar{E}_m dV}{(k_m^2 - n^2 k^2) \int_V |\bar{E}_m|^2 dV} - \frac{jn\omega\epsilon}{(k_m^2 - n^2 k^2)} \frac{\oint_S (\hat{n} \times \bar{E}_n) \cdot \bar{H}_m dS}{\int_V |\bar{H}_m|^2 dV} \right] \bar{H}_m
\end{aligned} \tag{A5}$$

Because we used Stokes' theorem, we have gone to a closed surface S , which leaves the metal and cuts across the waveguide (and transversely across the beam pipe) sufficiently far from the cavity that only the normal waveguide fields are present. We have also introduced the drive wavenumber $k = \omega/c$.

As expected, the field solutions are specified completely by the current source term and the electric field at the boundary.

The tangential electric field on the metal satisfies

$$\hat{n} \times \bar{E}_m = -\sqrt{\frac{n\omega\mu}{2\sigma}} (1+j) \bar{H}_m \tag{A6}$$

Thus (using $\hat{n} \cdot \bar{H}_m = 0$ on Σ),

$$\frac{\oint_S (\hat{n} \times \bar{E}_n) \cdot \vec{\nabla} \times \bar{E}_m d\Sigma}{\int_V |\bar{E}_m|^2 dV} = -\frac{\oint_S k_m K_{m,n} \sqrt{\frac{n\omega\mu}{2\sigma}} (1+j) \bar{H}_m \cdot \bar{H}_m d\Sigma}{\int_V |\bar{H}_m|^2 dV} \tag{A7}$$

because the earlier normalization is equivalent to

$$\int_V |\bar{E}_m|^2 dV = \int_V |\bar{H}_m|^2 dV \tag{A8}$$

Using

$$\frac{\oint_{\Sigma} \bar{H}_m \cdot \bar{H}_m d\Sigma}{\int_V |\bar{H}_m|^2 dV} = \frac{n\omega\mu}{Q_m \sqrt{\frac{n\omega\mu}{2\sigma}}} \quad (A9)$$

where Q_m is the unloaded cavity Q for mode m , the above integral is just

$$-k_m K_{m,n} \frac{n\omega\mu}{Q_m} (1+j) \quad (A10)$$

The surface integral over the waveguide cross section is

$$\frac{\oint_{S-\Sigma} (\hat{n} \times \bar{E}_n) \cdot \bar{\nabla} \times \bar{E}_m dS}{\int_V |\bar{E}_m|^2 dV} = -\frac{n\omega\mu}{Q_{m,ext}} k_m K_{m,n} \quad (A11)$$

where $Q_{m,ext}$ is the cavity Q loaded by the external waveguide for mode m . Likewise,

$$\frac{\oint_S (\hat{n} \times \bar{E}_n) \cdot \bar{H}_m dS}{\int_V |\bar{H}_m|^2 dV} = -n\omega\mu K_{m,n} \left(\frac{1+j}{Q_m} + \frac{1}{Q_{m,ext}} \right) \quad (A12)$$

We can identify $D_{m,n}$ and $K_{m,n}$ from Eqn. (A5), and using Eqns. (A10) - (A12), we have

$$D_{m,n} = \frac{k_m K_{m,n}}{(k_m^2 - n^2 k^2)} \left(\frac{1+j}{Q_m} + \frac{1}{Q_{m,ext}} \right) - \frac{j n \omega \mu}{(k_m^2 - n^2 k^2)} \frac{\int_V \bar{J}_n \cdot \bar{E}_m dV}{\int_V |\bar{E}_m|^2 dV} \quad (A13)$$

$$K_{m,n} = \frac{k_m}{(k_m^2 - n^2 k^2)} \frac{\int_V \bar{J}_n \cdot \bar{E}_m dV}{\int_V |\bar{E}_m|^2 dV} + \frac{j n^2 \omega^2 \epsilon \mu K_{m,n}}{(k_m^2 - n^2 k^2)} \left(\frac{1+j}{Q_m} + \frac{1}{Q_{m,ext}} \right)$$

Solving for $K_{m,n}$ first and then for $D_{m,n}$ gives

$$\begin{aligned}
D_{m,n} &= \frac{n\omega\mu}{j} \frac{\int_V \vec{J}_n \cdot \vec{E}_m dV}{\int_V |\vec{E}_m|^2 dV} \frac{1 + \frac{1}{Q_m} - \frac{j}{Q_m} - \frac{j}{Q_{m,\text{ext}}}}{k_m^2 - n^2 k^2 \left(1 + \frac{1}{Q_m} - \frac{j}{Q_m} - \frac{j}{Q_{m,\text{ext}}} \right)} \\
&= -n\omega\mu \frac{\int_V \vec{J}_n \cdot \vec{E}_m dV}{\int_V |\vec{E}_m|^2 dV} \frac{1}{\bar{k}_m^2 \left(\frac{1/Q_m + 1/Q_{m,\text{ext}}}{1 + 1/Q_m} \right) + j(n^2 k^2 - \bar{k}_m^2)} ,
\end{aligned} \tag{A14}$$

where we have defined a loaded-cavity resonant wavenumber (and related frequency) to be

$$\bar{k}_m^2 = k_m^2 \frac{1 + 1/Q_m}{(1 + 1/Q_m)^2 + (1/Q_m + 1/Q_{m,\text{ext}})^2} . \tag{A15}$$

We can define a shunt impedance for mode m to be (dropping the earlier subscript notation)

$$R_m = \frac{\left(\int \vec{E}_m(r) \cdot d\vec{l} \right)^2}{2P_{m,\text{dis}}} , \tag{A16}$$

where the line integral is taken along the same path we choose for defining our gap voltage and $P_{m,\text{dis}}$ is the power dissipated in the cavity walls for mode m . Since the gap voltage of mode m generated from the n^{th} harmonic of the current is

$$V_{\text{gap } m,n} = D_{m,n} \int \vec{E}_m(r) \cdot d\vec{l} \tag{A17}$$

we can rewrite Eqn. (A14) defining a cavity impedance for mode m and harmonic n ,

$$\begin{aligned}
V_{\text{gap } m,n} &= -\frac{\int_V \vec{J}_n \cdot \vec{E}_m dV}{\int \vec{E}_m(r) \cdot d\vec{l}} Z_{\text{cav } m,n} \\
&= -\frac{\int_V \vec{J}_n \cdot D_{m,n} \vec{E}_m dV}{V_{\text{gap } m,n}} Z_{\text{cav } m,n} .
\end{aligned} \tag{A18}$$

The total gap voltage is then

$$V_{\text{gap}} = \sum_{m,n} -\frac{\int_V \vec{J} \cdot \vec{E}_m dV}{\int \vec{E}_m(r) \cdot d\vec{l}} Z_{\text{cav } m,n} e^{jn\omega t} . \quad (\text{A19})$$

We can define an induced current for the n^{th} harmonic of mode m as

$$i_{\text{ind } m,n} = -\frac{\int_V \vec{J}_n \cdot \vec{E}_m dV}{V_{\text{gap } m,n}} . \quad (\text{A20})$$

The total gap voltage is then given by

$$V_{\text{gap}} = \sum_{m,n} i_{\text{ind } m,n} Z_{\text{cav } m,n} e^{jn\omega t} \quad (\text{A21})$$

and we have proven Ramo's theorem under Fourier decomposition for arbitrary cavity external coupling (the minus sign arises from the direction of the line integral for the gap voltage). The cavity impedance is given by

$$\frac{1}{Z_{\text{cav } m,n}} = \frac{\omega_m^2}{n^2 \omega^2} \left[\left(\frac{\frac{1}{Q_m} + \frac{1}{Q_{m,\text{ext}}}}{1 + \frac{1}{Q_m}} \right) \frac{Q_m}{R_m} + j \left(\frac{n\omega}{\bar{\omega}_m} - \frac{\bar{\omega}_m}{n\omega} \right) \frac{\frac{n\omega}{\bar{\omega}_m}}{\frac{R_m}{Q_m}} \right] . \quad (\text{A22})$$

We immediately see that this impedance can be represented by the circuit model in Fig. 5 with the correct choices of impedance, capacitance and inductance. Thus, we are physically justified in using the parallel circuit model to represent a cavity driven by a beam. We can take the no-external coupling and large-external coupling limits of Eqn. (A22) to gain some physical insight. First, we assume that the cavity will be driven close to the loaded resonance of the desired mode, $n\omega \approx \bar{\omega}_m$, which makes the term that modifies the R/Q term unity. We will also assume that Q_m is large. In the no-external coupling limit, $\omega_m \approx \bar{\omega}_m$, and we find that the cavity impedance reduces exactly to the usual form used in Section IV,

$$\frac{1}{Z_{\text{cav } m,n \text{ no ext}}} = \frac{1}{R_m} + j \left(\frac{n\omega}{\bar{\omega}_m} - \frac{\omega_m}{n\omega} \right) \frac{1}{\frac{R_m}{Q_m}} . \quad (\text{A23})$$

The cavity impedance in the large-external coupling limit is

$$\frac{1}{Z_{\text{cav } m,n \text{ ext}}} = \left[1 + \frac{1}{Q_{m,\text{ext}}^2} \right] \left[\frac{Q_m}{Q_{m,\text{ext}}} \frac{1}{R_m} + j \left(\frac{n\omega}{\bar{\omega}_m} - \frac{\bar{\omega}_m}{n\omega} \right) \frac{1}{R_m} \frac{Q_m}{Q_{m,\text{ext}}} \right]. \quad (\text{A24})$$

We notice several interesting features in this limit. First, the cavity R/Q term is basically unmodified, and also the shunt impedance term scales with the loaded cavity Q , as we would expect. Additionally, the first bracketed term suggests that the cavity shunt impedance is decreased as the external coupling becomes large. For a given induced current, this factor reduces the gap voltage. It also reduces the power in the cavity as well as the power extracted from the cavity.

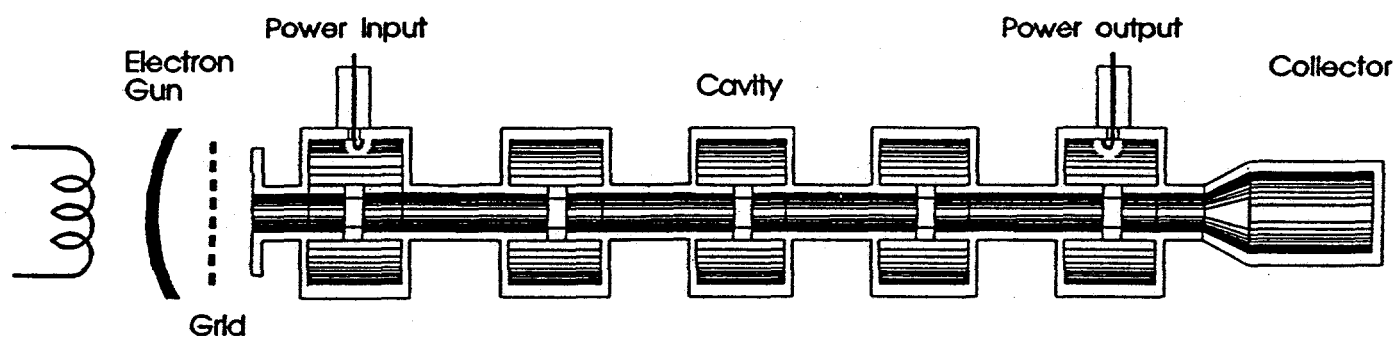
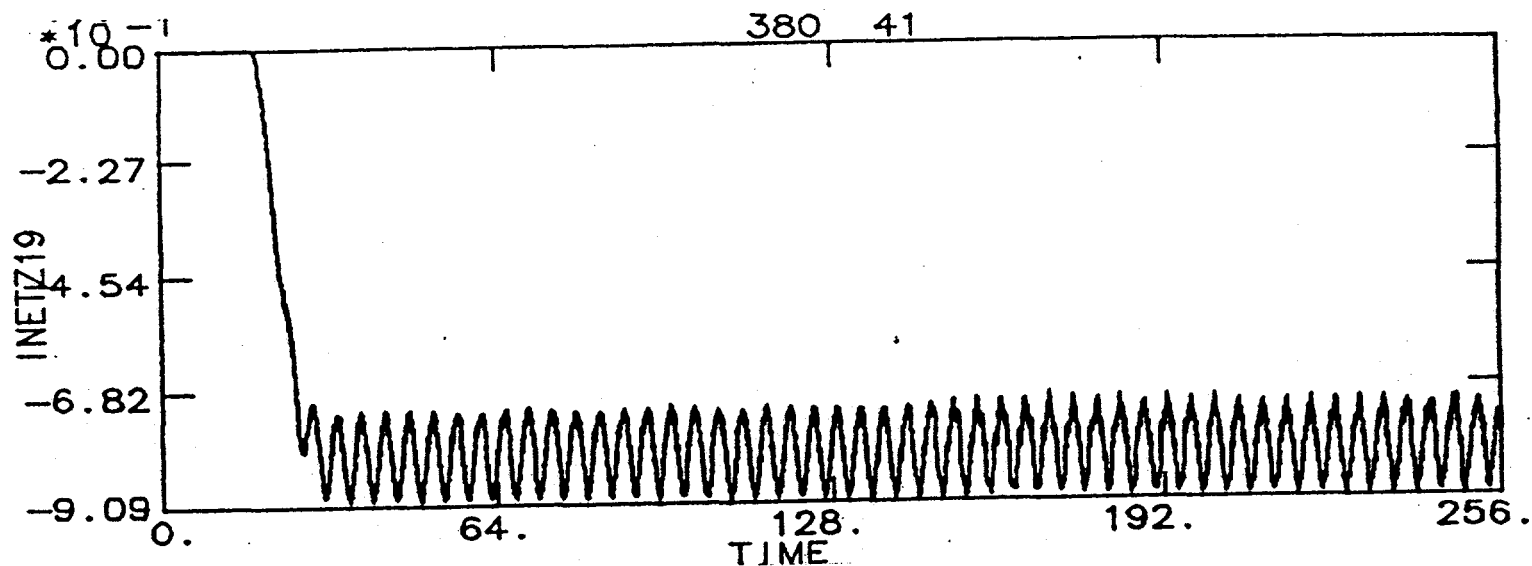
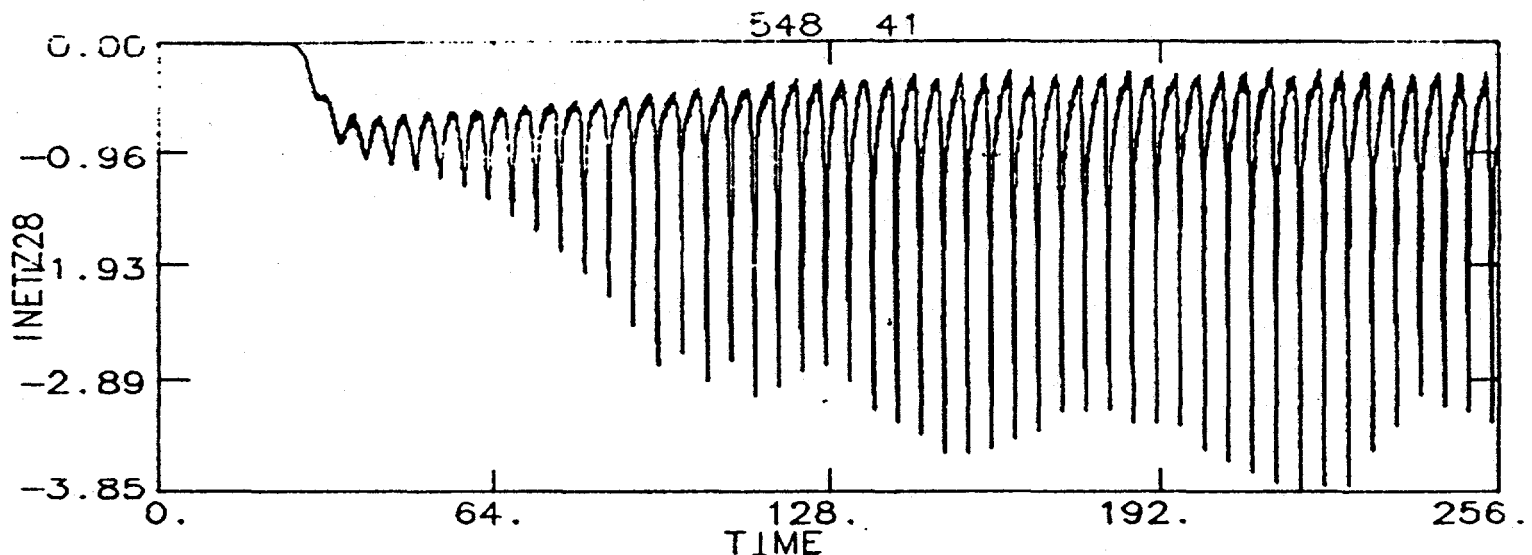


FIG. 1

Multi-cavity klystron schematic (from Power Klystrons Today, by Smith and Phillips, Research Studies Press, LTD).



(a) 11% harmonic current (average current is about 0.81 on this scale)



(b) 76% harmonic current (average current is about 0.81 on this scale)

FIG. 2 Sample numeric current profiles

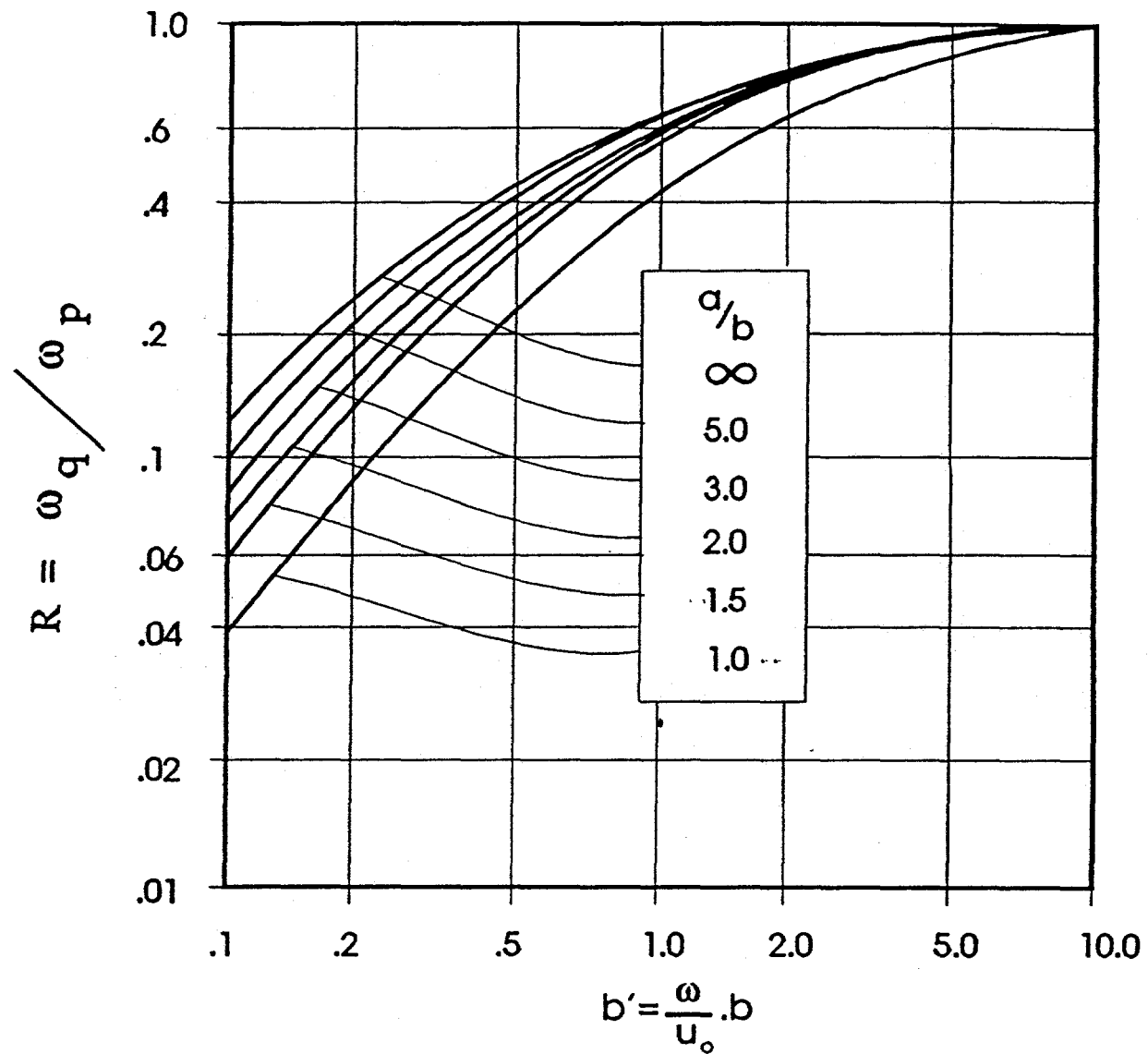


FIG. 3

Space-charge reduction factor for a solid beam (from Power Klystrons Today, by Smith and Phillips, Research Studies Press, LTD).

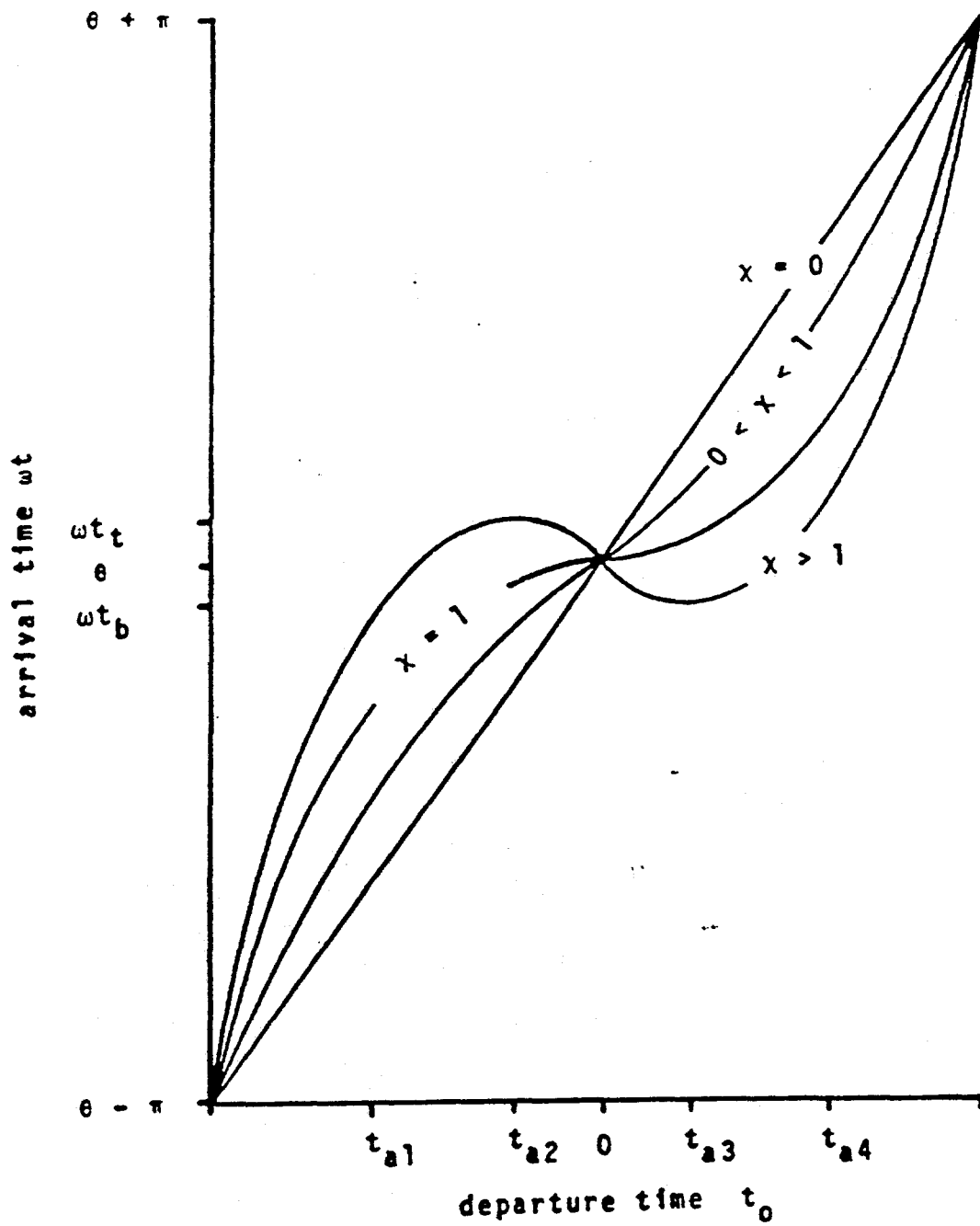


FIG. 4

Arrival time t versus exit time t_0 for ballistic motion after a gridded gap. The values t_l , t_b , t_{a1} , t_{a2} , t_{a3} , and t_{a4} show how the time integrals will be broken up when the exit time is multi-valued.

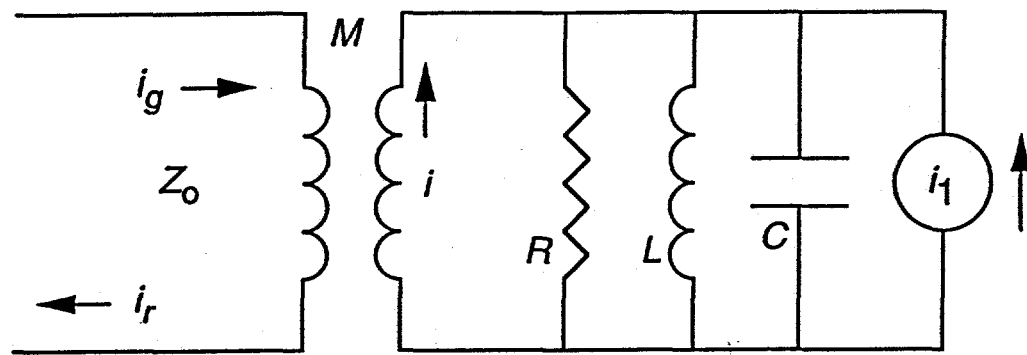


FIG. 5

Equivalent circuit of a klystron cavity, including an external drive, using the induced current defined in Eqn. (42) to describe the influence of a bunched electron beam.

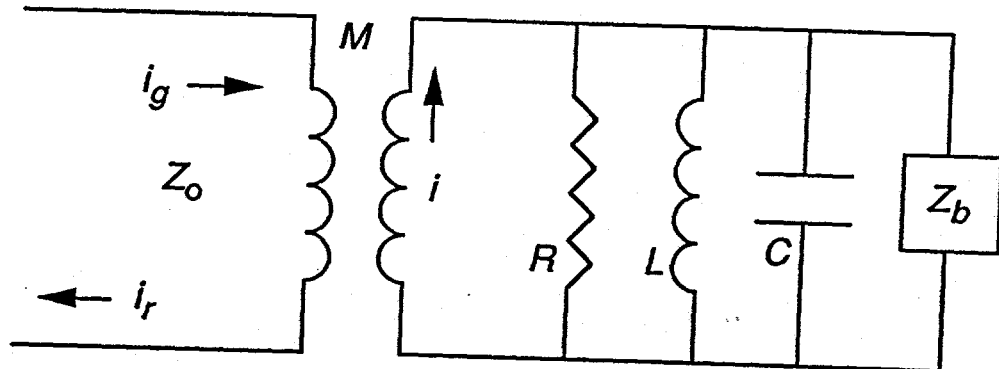


FIG. 6

Equivalent circuit of a klystron cavity, including an external drive, using the beam impedance defined in Eqn. (53) to describe the influence of a bunched electron beam.

DISCLAIMER

This report was prepared as an account of work sponsored by an agency of the United States Government. Neither the United States Government nor any agency thereof, nor any of their employees, makes any warranty, express or implied, or assumes any legal liability or responsibility for the accuracy, completeness, or usefulness of any information, apparatus, product, or process disclosed, or represents that its use would not infringe privately owned rights. Reference herein to any specific commercial product, process, or service by trade name, trademark, manufacturer, or otherwise does not necessarily constitute or imply its endorsement, recommendation, or favoring by the United States Government or any agency thereof. The views and opinions of authors expressed herein do not necessarily state or reflect those of the United States Government or any agency thereof.